

Spacetime structure of self-similar spherically symmetric perfect fluid solutions

B. J. Carr

Astronomy Unit, Queen Mary, Mile End Road, London E1 4NS, UK

Carsten Gundlach

Faculty of Mathematical Studies, University of Southampton, Southampton SO17 1BJ, UK

(Dated: 4.12.02)

We classify all spherically symmetric and homothetic spacetimes that are allowed *kinematically* by constructing them from a small number of building blocks. We then restrict attention to a particular *dynamics*, namely perfect fluid matter with the scale-free barotropic equation of state $p = \alpha\mu$ where $0 \leq \alpha < 1$ is a constant. We assign conformal diagrams to all solutions in the complete classification of Carr and Coley, and so establish which of the kinematic possibilities are realized for these dynamics. We pay particular attention to those solutions which arise as critical solutions during gravitational collapse.

Contents

I. Introduction	1
II. Kinematics of spherically symmetric and homothetic spacetimes	2
III. Perfect fluid matter	3
IV. Causal structure of perfect fluid CSS solutions	5
A. Asymptotically Friedmann solutions	5
B. Asymptotically quasi-static solutions	6
C. The asymptotically Minkowski solutions with $\alpha > \frac{1}{5}$	8
D. Asymptotic Kantowski-Sachs solutions	9
V. Critical solutions and shocks	10
VI. Conclusions	12
Acknowledgments	13
A. The sonic surface	13
B. Asymptotically Minkowski type B	13
References	14

I. INTRODUCTION

Self-similar and spherically symmetric solutions play an important role in many areas of physics. In Newtonian

physics, using suitable space and time coordinates \vec{x} and t , self-similarity is an ansatz $f(\vec{x}, t) = f_0(\vec{x}/t)$ for some field f that is of interest. On the one hand, such an ansatz simplifies the field equations by eliminating one coordinate. (In spherical symmetry, in particular, the self-similar ansatz simplifies field equations that are partial differential equations in r and t to ordinary differential equations in one variable r/t .) On the other hand, self-similar solutions are often attractors, or intermediate attractors, and are therefore good approximations to *generic* solutions during some stage of their evolution.

A classic example is the solution of the Riemann problem in 1-dimensional fluid dynamics, where at $t = 0$ the fluid has one constant velocity, density and entropy for $x < 0$, and another set of constant values for $x > 0$. The resulting shock solution is self-similar in the coordinate x/t . The reason for self-similarity is that the initial data do not contain any length scale. The self-similar solution is a good approximation over an intermediate range of scales, larger than the molecular scale where the fluid assumption breaks down but smaller than the scale on which the solution varies smoothly.

In general relativity, the most common definition of self-similarity is homotheticity: the spacetime admits a vector field ξ^μ with the property that the Lie-derivative of the metric along this field is a constant times the metric:

$$\mathcal{L}_\xi g_{\mu\nu} = -2g_{\mu\nu}. \quad (1)$$

(The choice of the constant as -2 is a convention, the negative sign being chosen so that ξ^μ points towards increasing curvature.) This definition expresses the scale-invariance of the spacetime metric, and is analogous to the Newtonian notion of self-similarity. With spherical symmetry, it is possible to introduce coordinates t and r so that all metric coefficients depend only on r/t . In general relativity, self-similarity has an important application in gravitational collapse: during collapse whose initial data are close to the black hole threshold, certain self-similar “critical” solutions act as universal intermediate attractors

The continuous self-similarity (CSS) that we have discussed already can be generalized to a discrete self-similarity (DSS), in which $f(\vec{x}, t)$ depends arbitrarily on \vec{x}/t but can also depend on $\ln|t|$ in a periodic manner, with some period Δ . Clearly such solutions are scale-periodic rather than scale-invariant. Several known critical solutions in gravitational collapse, in particular those with scalar field matter and in vacuum gravity, are DSS rather than CSS. In this paper we are interested in perfect fluids, where the critical solutions are CSS, and from now on we restrict our discussion to this case. We refer to CSS when we specifically mean the continuous symmetry, and to self-similarity in any statements that are also true for DSS.

We proceed in three steps. We first discuss the kinematic consequences of CSS in spherical symmetry, generalizing the discussion in Ori and Piran [1] and Nolan [2]. We then discuss the dynamics with perfect fluid matter and examine which of the kinematic possibilities are realized dynamically. We assume the linear barotropic equation of state $p = \alpha\mu$, which is the only one that is compatible with exact self-similarity. We use the classification by Carr and Coley [3] of all spherically symmetric CSS perfect fluid solutions to draw the corresponding conformal diagrams. Finally, we look more closely at those solutions that appear as critical solutions in gravitational collapse.

II. KINEMATICS OF SPHERICALLY SYMMETRIC AND HOMOTHETIC SPACETIMES

In this section we discuss the kinematics of spherical symmetry, without using the Einstein equations. Any spherically symmetric spacetime is naturally the product of a two-dimensional reduced spacetime M^2 crossed with the 2-sphere S^2 . Any point in the reduced spacetime corresponds to a 2-sphere of area $4\pi R^2$. Here R transforms as a scalar on the reduced spacetime, and $R = 0$ is a boundary of the reduced spacetime, which can either be a regular center or a central curvature singularity. A local mass function m can be defined by $1 - (2m/R) \equiv \nabla_\mu R \nabla^\mu R$. Any point in the reduced spacetime where $\nabla_\mu R$ is timelike is a closed trapped surface in the full spacetime and a surface where $\nabla_\mu R$ is null is called an apparent horizon.

We now restrict attention to spherically symmetric CSS spacetimes. The integral curves of the homothetic vector field (homothetic lines) provide a natural fibration of the 4-dimensional spacetime, and therefore a natural foliation of the reduced spacetime. Labelling the integral curves provides a natural global coordinate on the reduced spacetime, which we shall call z . In this paper we construct conformal diagrams for the reduced spacetime. Apart from any singularities and conformal boundaries, lines of geometric significance include the homothetic lines, the lines of constant R and the fluid world

lines.

We shall describe two building blocks from which any spherically symmetric CSS spacetime can be built. Our arguments in this section are purely kinematic. They are therefore valid for any matter. On the other hand, for a given type of matter not every spacetime that can be assembled from the building blocks can be realized as a solution of the field equations. We illustrate this in Section IV for perfect fluid matter.

The key kinematic consequence of self-similarity in general relativity is the existence of a strong curvature singularity. It can be shown from (1) that in the direction ξ^μ any homothetic line runs into a curvature singularity in finite proper time, proper distance or affine parameter distance s , unless the curvature vanishes identically on the curve [4, 5]. If the origin of s is chosen so that the singularity is at $s = 0$, the Kretschmann scalar scales as s^{-4} , the Ricci scalar as s^{-2} and the mass as s^{-1} . Every homothetic line is infinitely extended in the direction $-\xi^\mu$ (i.e. with increasing s).

Any homothetic spacetime has therefore the manifold structure of the half-line $0 < s < \infty$ crossed with an interval in z (which can be finite or infinite). $s = 0$ is always a curvature singularity and $s = \infty$ is always a physical infinity. The boundaries $z = z_{\min}$ and $z = z_{\max}$ can be either regular centers or central singularities. The manifold structure is shown in Fig. 1. It is important to note that this on its own does not determine the causal structure, but it does mean that all components of the singularity are connected. The usual conformal diagram of a closed Friedmann universe with disjoint big bang and big crunch singularities, for example, cannot be realized in a spherically symmetric CSS spacetime. Nevertheless, fluid world lines can begin on one section of the singularity (big bang) and end on another (black hole/big crunch). The difference is that in a spherically symmetric CSS solution these two components of the singularity must be connected either directly or through a null singularity.

We obtain our two building blocks from considering radial null geodesics that are also homothetic lines. Ori and Piran [1] call such a line a *simple* radial null geodesic (SRNG). Assuming that the spacetime contains an isolated SRNG, with neighboring homothetic lines are timelike on one side of the SRNG and spacelike on the other, there are two possibilities: either the homothetic lines converge with respect to radial null geodesics as they approach the singularity at $s = 0$ or they diverge.

The first possibility is illustrated in Fig. 2. We call this building block a “fan”. The homothetic lines converge as $s \rightarrow 0$. The singularity $s = 0$, for an interval of z , is then just a single point. Any non-simple radial null geodesic is given by $z = z(s)$. It is clear from the figure that $z(s)$ is repelled from z_0 on either side as $s \rightarrow 0$. Conversely, $z(s)$ is attracted to z_0 as $s \rightarrow \infty$. ($z = z_0, s = \infty$) is therefore not a point but an extended piece of null

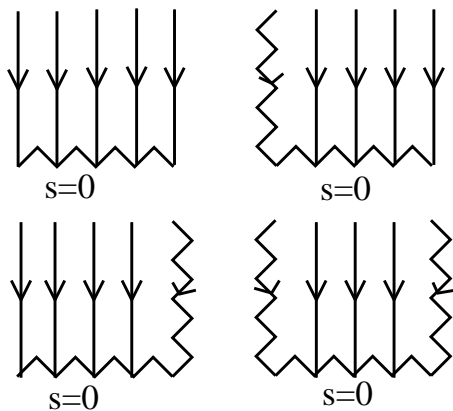


FIG. 1: The manifold structure of any spherically symmetric self-similar spacetime: an interval $z_{\min} \leq z \leq z_{\max}$ times the half-line $0 < s < \infty$. Note that this diagram is *not* a conformal diagram: although $s = 0$ is shown here as a horizontal line, it could be a single point or a line with spacelike, timelike or null segments. Homothetic lines $z = \text{const.}$ are shown bold with arrows that point to the singularity $s = 0$. The four cases where none, one or both of the limits $z = z_{\min}$ and z_{\max} are singularities are shown.

infinity. In summary, the spacetime contains a fan when it contains a SRNG $z = z_0$ such that $z(s)$ for non-simple radial null geodesics approaches z_0 as $s \rightarrow \infty$, that is it obeys $[z(s) - z_0] dz/ds < 0$. A fan implies a point singularity at $s = 0$ for a finite range of z , and a null infinity at $(s = \infty, z = z_0)$.

The opposite structure is illustrated in Fig. 3. Here the non-simple radial null geodesics $z = z(s)$ approach $z = z_0$ as $s \rightarrow 0$, and are repelled from z_0 as $s \rightarrow \infty$. Therefore the singularity ($z = z_0, s = 0$) is reached not just by one but many radial null geodesics, and so it is a null line. Conversely, $s = \infty$ for a range of z on each side of z_0 is a just a single point, rather than an extended piece, of null infinity. We call this structure a “splash” because the homothetic line $z = z_0$ runs into the singularity at $s = 0$ and then bifurcates to form the null singularity. The spacetime contains a splash when it contains a SRNG $z = z_0$ such that $z(s)$ for non-simple radial null geodesics approaches z_0 as $s \rightarrow 0$. A splash implies a null central singularity at $s = 0$.

Note that the coordinates s and z break down at both $s = 0$ and $s = \infty$ in a fan or splash. Regular double null coordinates for a fan and a splash are constructed in [5]. (This construction also proves that the singularity $s = 0$ in a splash is null, a fact which was asserted but not proved in [1] and [2].) Note also that in principle the homothetic lines could be timelike (or spacelike) on *both* sides of the SNRG. In this case, one would only have the upper (or lower) half of the diagrams shown in Fig. 2 and Fig. 3, corresponding to what one might term a “semi-fan” or “semi-splash” respectively. However, we do not show the corresponding figures explicitly.

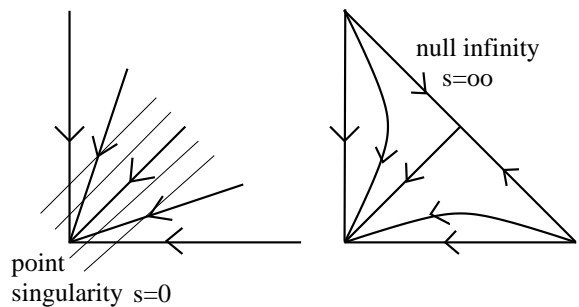


FIG. 2: A fan: a range of homothetic lines meet in a point on the singularity. Homothetic lines are shown bold with arrows that point to the singularity, in the direction ξ^μ . One of them, $z = z_0$, is also a radial null geodesic (a SRNG). Four other (non-simple) radial null geodesics $z = z(s)$ are shown as thin lines. The conformal diagram on the left is not compactified. On the right, the same conformal diagram has been compactified to show that $(z = z_0, s = \infty)$ is a piece of null infinity.

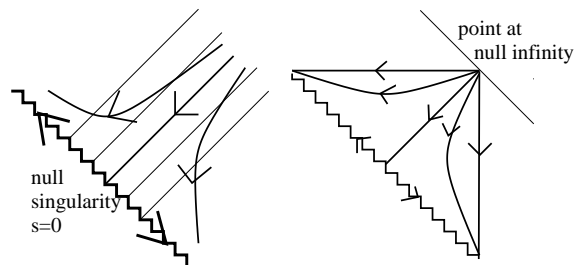


FIG. 3: A splash: A SRNG $z = z_0$ is flanked by homothetic lines that diverge from it as the singularity is approached. Homothetic lines $z = \text{const.}$ are shown bold with arrows that point to the singularity. The SNRG branches and runs along the singularity. The singularity $s = 0$ is null and is at finite distance. The conformal diagram on the left is not compactified. The conformal diagram on the right is compactified to show that a range of homothetic lines meet in a point at null infinity.

III. PERFECT FLUID MATTER

We now examine spherically symmetric CSS spacetimes with perfect fluid matter with the equation of state $p = \alpha\mu$, where p is the pressure, μ is the total energy density, and $0 \leq \alpha < 1$ is a constant. We briefly introduce notation based on [3] and [6]. The metric is given in comoving coordinates by

$$ds^2 = -e^{2\nu} dt^2 + e^{2\lambda} dr^2 + R^2 d\Omega^2, \quad (2)$$

where $0 \leq r < \infty$ labels fluid worldlines. The fluid velocity is therefore $U^\mu = (e^{-\nu}, 0, 0, 0)$. Spherically symmetric CSS solutions can be put into a form in which all dimensionless quantities are functions only of the dimensionless self-similar variable $z = r/t$. In particular, we enforce homotheticity by demanding that

$$\nu(t, r) = \nu(z), \quad \lambda(t, r) = \lambda(z),$$

$$R(t, r) = rS(z), \quad 8\pi G\mu(t, r) = r^{-2}\eta(z). \quad (3)$$

The homothetic vector defined by (1) is

$$\xi^\mu \frac{\partial}{\partial x^\mu} = -t \frac{\partial}{\partial t} - r \frac{\partial}{\partial r} \quad (4)$$

in these coordinates. Varying z for a given t specifies the spatial profile of various quantities. For a given value of r (i.e., for a given fluid element), it specifies their time evolution. The remaining gauge-freedom in CSS solutions corresponds to a scaling of the r and t coordinates.

Two quantities have special physical significance [3]. The first is the CSS mass function, which is defined in terms of the Hawking mass $m(r, t)$ and the area radius $R(t)$:

$$M(z) = \frac{m}{R}. \quad (5)$$

One has an apparent horizon wherever $M = 1/2$. The second is the CSS velocity function

$$V(z) = e^{\lambda-\nu} z, \quad (6)$$

which represents the velocity of the spheres of constant z relative to the fluid. In geometric terms,

$$\frac{\xi^\mu u_\mu}{\sqrt{\xi^\nu \xi_\nu}} = \frac{1}{\sqrt{1-V^2}}. \quad (7)$$

This should not be confused with the velocity of the fluid with respect to the lines of constant R , the ‘‘radial 3-velocity’’, which we denote by V_R . Special significance is attached to values of z for which $|V| = \sqrt{\alpha}$ and $|V| = 1$. The first corresponds to a sonic point, the second to a black-hole event horizon or a cosmological particle horizon. A useful relation is that for radial null geodesics

$$d \ln r = \frac{d \ln z}{1 \pm V(z)}, \quad (8)$$

where the + and - signs correspond to ingoing and outgoing geodesics, respectively. This again shows that lines $z = z_0$ where $V(z_0) = \pm 1$ are both radial null geodesics and homothetic lines, that is they are SRNGs.

It should be noted that finite values of z sometimes correspond to zero or infinite R and zero values of z sometimes correspond to non-zero R . Also some solutions span both negative and positive values of t , which means that $z = r/t$ jumps from $-\infty$ to $+\infty$. (This occurs at $t = 0$, which is the homothetic line orthogonal to the fluid worldlines.)

Two of the Einstein equations can be solved in closed form to give ν and λ in terms of z , $S(z)$ and $\eta(z)$. One then obtains a second-order ODE for S and a first-order ODE for η in the independent variable z . The equation for d^2S/dz^2 can be written as two first-order equations for dS/dz and dM/dz . One then obtains the system

$$\frac{dM}{dz} = a(S, M, \eta, z), \quad (9)$$

$$\frac{dS}{dz} = b(S, M, \eta, z), \quad (10)$$

$$\frac{d\eta}{dz} = \frac{g(S, M, \eta, z)}{V^2(S, \eta, z) - \alpha}, \quad (11)$$

subject to the constraint

$$c(S, M, \eta, z) = 0. \quad (12)$$

Here a , b , c , V^2 and g are known regular functions of M , S , η and the independent variable z . The constraint can in principle be used to eliminate z from the right-hand sides, so that one obtains a 3-dimensional dynamical system. Therefore, for a given value of α , the space of solutions is locally 2-dimensional. In practice the constrained and non-autonomous form is retained for calculations.

Points where $V = \pm\sqrt{\alpha}$ need particular attention. In phase space the condition $V^2 = \alpha$ corresponds to a 2-dimensional surface, which we call the *sonic surface*. Eqn (10) implies that solutions can be continued through the sonic surface only on the 1-dimensional line in phase space where both $V^2 = \alpha$ and $g = 0$; we call this the *sonic line*. We use the term *sonic point* for the 3-dimensional surface in spacetime where $V^2 = \alpha$.

The details are summarized for completeness in Appendix A. Here we discuss the effect that the existence of sonic points has on the local dimensionality of the solution space. The sonic line can be divided into three parts. It has a ‘‘focal’’ segment that cannot be crossed by any solution curves and is a repeller. It also has a ‘‘saddle segment’’, each point of which is crossed by two isolated analytic solutions. Finally, it has two ‘‘node’’ segments, each point of which is crossed by a 1-parameter family of C^1 solutions and an isolated solution. All the C^1 solutions are tangential to each other at the sonic line. Therefore, if one does not require the solution to be analytic, any of the C^1 solutions on one side of the sonic surface can be continued by any of the C^1 solutions on the other side. Like a saddle, a node is also crossed by two analytic solutions. One of these is a member of the C^1 family, while the other is the isolated solution.

The global dimensionality of the families of solutions that we discuss below can be determined as follows. If z_{\min} is a singularity, the space of solutions locally has two free parameters. If it is a regular center, it obeys one condition and so the solution locally has only one free parameter. If the solution crosses the sonic point analytically (i.e. at a node or a saddle), it loses one parameter. For example, critical solutions have a regular center and are analytic at the sonic point, so there are no free parameters, indicating that there are at most isolated solutions with those properties. On the other hand, if the solution crosses a node as a C^1 solution, the continuation is not unique and so gains one parameter. The same argument applies to any subsequent sonic point.

Note that the presence of a sonic point cannot be inferred from the conformal diagrams presented below. Each

sonic point is a timelike homothetic line, but a region in which the homothetic lines are timelike need not contain a sonic point.

IV. CAUSAL STRUCTURE OF PERFECT FLUID CSS SOLUTIONS

Carr and Coley [3] (from now on CC) classify solutions in terms of their behavior in the asymptotic limit $|z| \rightarrow \infty$, since this can only take one of a few simple forms: asymptotically Friedmann, asymptotically Kantowski-Sachs, what they term asymptotically ‘quasi-static’, and asymptotically Minkowski. There is also a family which asymptotes to the Minkowski form at finite z because $R \rightarrow \infty$ there. In the conformal diagram, all these asymptotic behaviors are associated with the region near i^o . CC also discuss the behavior of solutions in the limit $z \rightarrow 0$ and find that they are either exactly static or asymptotically Friedmann (corresponding to a ‘regular’ origin). There are also solutions which have their origin at finite z because $R \rightarrow 0$ there, corresponding to a spacelike singularity. In the conformal diagram, these asymptotic behaviors are associated with the regions near i^+ or i^- .

CC place considerable emphasis on the form of the scale factor $S(z)$ since this specifies the physical behavior of the fluid elements. They also emphasize the form of the velocity function $V(z)$ since this identifies event and particle horizons, sonic points and physical singularities. Although the $V(z)$ representation does not yield a complete understanding of solutions – one is projecting solutions in a 3-dimensional space onto a particular 2-dimensional plane, so that many physically distinct solutions may be superposed – it uniquely specifies features relevant to the conformal structure. In particular, $|V| = 1$ corresponds to a null line and infinite $|V|$ corresponds to a singularity. Integrating Eq. (8) shows that the value of r at $V = 1$ generally diverges for any outgoing photon, so this corresponds to I^+ . Our strategy here is to present the form of the functions $S(z)$ and $V(z)$ for each of the types of solution and then to use these to construct the conformal diagram. We will also show some fluid lines and homothetic lines in each case.

Note that we can trivially set $t \rightarrow -t$ and hence $z \rightarrow -z$ in any CSS solution, and so obtain its time reverse. As a matter of convention, we shall present each solution in only one time orientation, with “big bang” singularities in the past and “black hole” singularities in the future. For example, Fig. 4 describes an open universe that starts with a big bang and expands forever. Turned upside down, the same solution describes gravitational collapse from a regular initial state [1].

Carr et al. [7, 8] (from now on CCGNU) classify solutions in terms of the global causal properties of the homothetic vector ξ^μ and this is particularly relevant

in constructing the conformal diagram. The solutions are found to have five possible forms. There are type-T solutions for which ξ^μ is always timelike; these develop a shock, since their orbits necessarily end at an irregular sonic point. There are type-S solutions for which ξ^μ always is spacelike; these always have $|V| > 1$ and include some asymptotically Friedmann and asymptotically quasi-static solutions. There are type-TS solutions, such as the flat Friedmann one, for which ξ^μ changes causality once. Finally there are type-TST, STST, and STSTS solutions with two, three and four causality changes, respectively.

Here we make this shorthand description more detailed by denoting the fans and splashes that separate the S and T regions by f and p. Finally we denote the two boundaries z_{\min} and z_{\max} by either r for a regular center or s for a singularity. Note that the upper case letters S and T denote regions, while the lower case letters f, p, r and s denote lines. All kinematically possible CSS spacetimes can be constructed systematically from an alphabet of six letters subject to the following rules: The first and last letter are r or s. The other letters are f, p, T, S. Capital letters and lower case letters must alternate.

A. Asymptotically Friedmann solutions

There are two 1-parameter families of asymptotically Friedmann solutions as $|z| \rightarrow \infty$, one with $z > 0$ and the other with $z < 0$. The parameter characterizing these solutions measures the underdensity or overdensity relative to the flat Friedmann solution and is also associated with the asymptotic energy E . The $z > 0$ solutions correspond to inhomogeneous models that start from an initial big bang singularity at $z = \infty$ ($t = 0$) and then, as z decreases, either expand to infinity or recollapse. The $z < 0$ solutions are just the time-reverse of these but we do not discuss them explicitly. Depending on the value of E , two qualitatively different types of solution can be distinguished:

- 1) All solutions which are underdense ($E > 0$) or insufficiently overdense ($E < 0$ but exceeding some negative critical value E_{crit}) reach the sonic surface at $V = \sqrt{\alpha}$. They have $V = 1$ at some point z_1 and this corresponds to the cosmological particle horizon. The solutions in this class are of type ST for $z > 0$ and are illustrated in Fig. 4. Those which reach the sonic line in the range of z corresponding to nodes may be attached to a subsonic ($V < \sqrt{\alpha}$) solution which is regular solution at the origin. These solutions are also described by a single parameter and this is a measure of the density at the origin $z = 0$, so the transonic solutions represent density fluctuations that grow at the same rate as the particle horizon. They are generally non-analytic at the sonic point. While there is a continuum of regular underdense solutions, regular overdense solutions only occur in narrow bands (with just

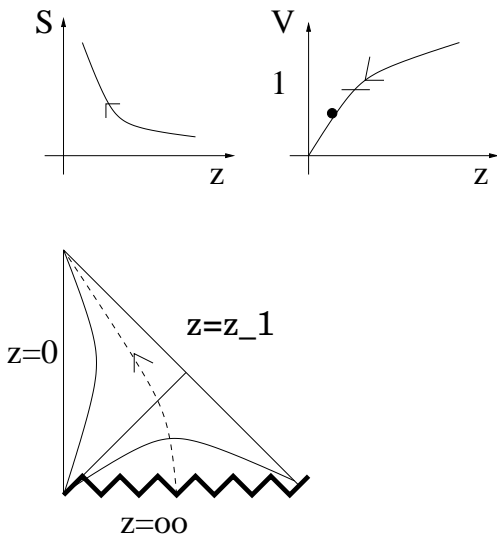


FIG. 4: The form of $S(z)$ and $V(z)$ for the asymptotically Friedmann solutions which expand forever, together with the conformal diagram. Homothetic lines are shown, together with a single fluid world line (shown broken). The arrows, here and in all diagrams that follow, indicate the direction of time. The causal structure is “singularity, region where the homothetic lines are spacelike, fan, timelike region, regular center”, or sSfTr in our shorthand notation.

one solution per band being analytic). The overdense solutions exhibit oscillations in the subsonic region and solutions with larger numbers of oscillations form ever narrower bands within the one-oscillation band (in terms of the ranges of z at the sonic line). The higher bands are all nearly static near the sonic point, although they depart from the static solution as they approach the origin. The conformal diagram for these solutions is essentially identical to that for flat Friedmann itself.

2) Solutions that are sufficiently overdense with respect to the flat Friedmann solution (i.e. for E less than the critical value E_{crit}) have the feature that V reaches a minimum and then rises again to infinity as z decreases to some finite value z_S . This indicates the formation of a singularity at which $S \rightarrow 0$ and $\mu \rightarrow \infty$ for finite a value of z . The solutions in this class are of type STS or S and are illustrated in Fig. 5 and Fig. 6, respectively. They correspond to black holes growing at the same rate as the Universe. [Note that the type STS solution with the smallest value of z_S is the one for which the minimum value of V is $1/\sqrt{\alpha}$ and this solution must touch the sonic surface at the value of z associated with the saddle/node transition.] Providing E exceeds some other critical value E_* , the minimum of V is below 1, as illustrated in Fig. 5, so there is a black-hole event horizon at z_2 and a cosmological particle horizon at z_1 where $V = 1$. However, it should be stressed that the conformal diagram is very different from that for a non-self-similar black hole in a flat Friedmann background. In particular, the black hole singularity is connected to the big bang singularity and

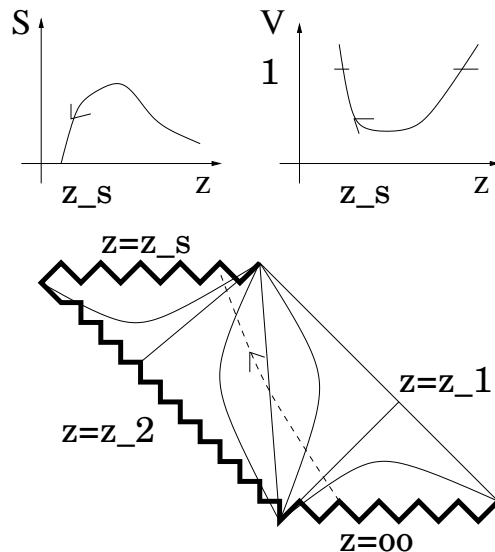


FIG. 5: The form of $S(z)$ and $V(z)$ for the asymptotically Friedmann solutions which contain a black hole with an event horizon, together with the conformal diagram. There is a fan at $z = z_{\text{ph}}$ and a splash at $z = z_{\text{eh}}$, and the causal structure is sSfTpSs.

necessarily naked for a while. For $E < E_*$, the minimum of V is above 1, as illustrated in Fig. 6, and the entire Universe is inside the black hole. (However, there is always an apparent horizon since CC show that the minimum of M is necessarily below $1/2$.) In this case, the conformal diagram has two spacelike singularities and there are no null infinities. This is because the integral over (8), for both signs, converges as $z \rightarrow \infty$ and $z \rightarrow z_S$, so any null geodesic covers only a finite range of $\ln r$ between the big bang singularity and the black hole/big crunch singularity. This contrasts with the conformal diagram for a recollapsing Friedmann universe, which has two separated spacelike singularities.

Note that when the minimum of V exactly equals 1, the conformal diagram in Fig. 5 loses the part in which the homothetic lines are timelike and so there is no longer a naked singularity. In terms of causal structure, the “fTp” part of Fig. 5 is replaced by a “semi-fan” and a “semi-splash”. However, the conformal diagram is still very different from the one shown in Fig. 6, so there is a qualitative change as the minimum of V passes through 1. In the cases discussed below, similar considerations apply whenever V has an extremum at ± 1 , but we will not comment on this explicitly.

B. Asymptotically quasi-static solutions

As discussed by CC, there is exactly one self-similar static solution for each value of α and a 1-parameter family of solutions that are asymptotically static (in the sense that

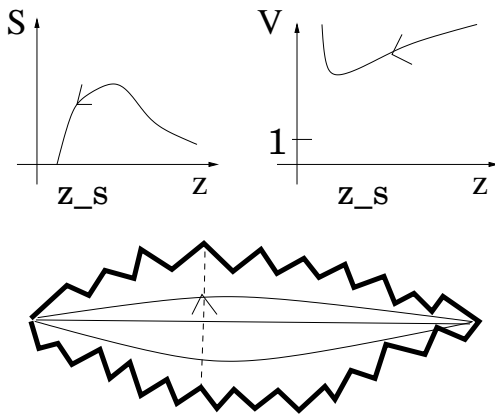


FIG. 6: The form of $S(z)$ and $V(z)$ for the asymptotically Friedmann solutions which contain a “universal” black hole, together with the conformal diagram. The causal structure is sSs, with no fan or splash, and homothetic lines are spacelike everywhere.

the radial 3-velocity V_R tends to zero as $|z| \rightarrow \infty$). There is also a 2-parameter family of solutions that are asymptotically “quasi-static” (in the sense that V_R is finite but not necessarily zero). However, it should be emphasized that the solutions in this class may only be close to the static solution for part of their evolution. One of the two parameters can be taken to be the asymptotic energy E , while the other (denoted by D) gives the value of z at the big bang or big crunch singularity. Note that D , unlike E and V_R , cannot be expressed explicitly in terms of the asymptotic parameters, so it is sometimes more convenient to use V_R as the second parameter.

The key feature of these asymptotically quasi-static solutions is that they span both negative and positive values of z and necessarily pass from $z = -\infty$ to $z = +\infty$, whereas the asymptotically Friedmann solutions are confined to $z > 0$ or $z < 0$ and are symmetric. This is because the big bang occurs at $z = -1/D$ (corresponding to a negative value of t) in these solutions, so the limit $|z| \rightarrow \infty$ has no particular physical significance. These solutions can be interpreted as inhomogeneous cosmological models with an advanced big bang. Equivalently, for the time-reversed solutions, there is a big crunch singularity at $z = +1/D$. There are two types of asymptotically quasi-static solutions. Those with E exceeding some negative critical value $E_{\text{crit}}(D)$ expand or collapse forever. Those with $E < E_{\text{crit}}(D)$ expand and then recollapse.

1) Ever-collapsing solutions. These start out from an infinitely dispersed state and describe the collapse of an inhomogeneous gas cloud to a singularity at $z = +1/D$ (i.e., after $t = 0$). (The ever-expanding solutions are just the time reverse of these and will not be considered explicitly.) They are of type TS or TSTS and illustrated in Fig. 7 and Fig. 8. They start with $V = 0$ at $z = 0$ and then, as z decreases, reach a sonic point where $V = \sqrt{\alpha}$. In this context, it should be noted that the second

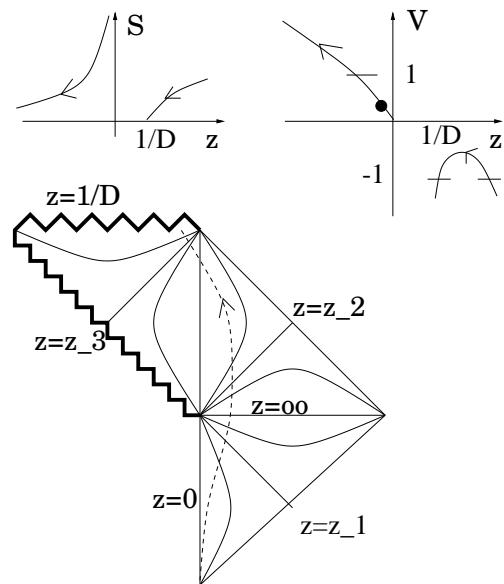


FIG. 7: The form of $S(z)$ and $V(z)$ for the ever-collapsing asymptotically quasi-static solutions which contain a naked singularity, together with the conformal diagram. The causal structure is rTfSfTpSs.

parameter D has relatively little effect on the form of the solutions in the subsonic regime. Indeed, all solutions apart from the exactly static one must be asymptotic to the flat Friedmann solution at small $|z|$. In particular, the models can collapse from infinity (i.e. $S \rightarrow \infty$ as $z \rightarrow 0$ or $t \rightarrow -\infty$) only if E is positive or lies in discrete bands if negative. The subsonic solution is then attached to a supersonic asymptotically quasi-static solution at the sonic line. The supersonic solutions pass through a Cauchy horizon at z_1 (where $V = 1$) before tending to the quasi-static form at $z = -\infty$ and jumping to $z = +\infty$. As z further decreases, V first reaches a maximum and then diverges to minus infinity when it encounters the singularity at $z = 1/D$. The maximum will be above -1 if E is less than some negative value $E_+(D)$ and there will then be two points z_2 and z_3 where $V = -1$. This case is illustrated in Fig. 7 and the conformal diagram is a combination of the one shown in Fig. 4 and Fig. 5. This shows that one necessarily has a naked singularity, as pointed out by Ori and Piran. The maximum of V will be below -1 for $E > E_+(D)$ and this case is illustrated in Fig. 8. The conformal diagram now resembles the one in Fig. 4, except that the singularity has $z = 1/D$ rather than an infinite value of z .

2) Expanding and recollapsing solutions. Solutions with E less than the critical value $E_{\text{crit}}(D)$ expand from an initial singularity in the $z < 0$ region and then recollapse to another singularity in the $z > 0$ region. They are of type S, STS or STSTS. The value of z is $-1/D$ at the initial singularity but depends on both E and D at the final one. As z decreases from $-1/D$, V rises from $-\infty$, reaches a maximum below $-\sqrt{\alpha}$ and then tends to the

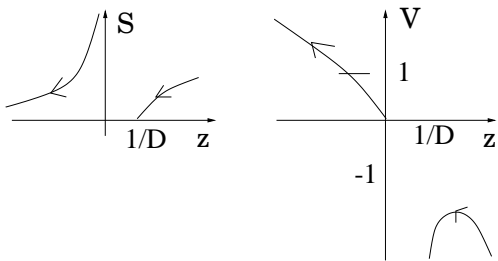


FIG. 8: The form of $S(z)$ and $V(z)$ for the ever-collapsing asymptotically quasi-static solutions which do not contain a naked singularity. The conformal diagram is the same as in Fig. 4, with structure sSfTr, although upside down.

quasi-static form as $z \rightarrow -\infty$. The solution then jumps to $z = +\infty$ and enters the $z > 0$ regime. As z continues to decrease, V decreases to a minimum above $\sqrt{\alpha}$ and then tends to $+\infty$ at the value of z corresponding to the recollapse singularity. We now have four possible situations, depending on whether the minimum of V is above or below $+1$ and whether the maximum of V is above or below -1 . If $V_{\max} > -1$ and $V_{\min} > 1$, one necessarily has a black-hole event horizon at z_1 and a cosmological particle horizon at z_2 in the $z < 0$ regime. This occurs if E exceeds some negative value $E_*(D)$ and the minimum of V will reach $\sqrt{\alpha}$ when E reaches $E_{\text{crit}}(D)$, corresponding to the last recollapsing solution. In this case, the solution is of the STS type and illustrated in Fig. 9. The conformal diagram just resembles that in Fig. 5, except that the initial singularity is at $z = 1/D$ rather than $z = \infty$, and this shows that the black hole singularity is necessarily naked. The case with $V_{\max} < -1$ and $V_{\min} < 1$ is equivalent to this and not shown explicitly. The case with $V_{\max} > -1$ and $V_{\min} < 1$ is of the STSTS type and illustrated in Fig. 10. There are now four points (z_1, z_2, z_3, z_4) at which $V = 1$ and so the conformal diagram is more complicated, though the singularity structure is unaltered. The case with $V_{\max} < -1$ and $V_{\min} > 1$ is illustrated in Fig. 11. There are now no points where $V = 1$ and so the conformal diagram is as in Fig. 6. In principle, there might be solutions with $E < E_{\text{crit}}(D)$ in which V has neither a maximum nor a minimum. However, such solutions would have two sonic points and parameter-counting suggests that it is unlikely that any solution having crossed the sonic surface once in a saddle could cross it again.

The exact static solution is illustrated in Fig. 12. The conformal diagram has the Minkowski form at large distance but there is a timelike naked singularity at the origin and points z_1 where $V = -1$ and z_2 where $V = 1$. Note that there are no solutions which are asymptotic to the static solution at $z = 0$ apart from the static solution itself, so there are no perturbations of the exact static solution. The asymptotically quasi-static solutions with a regular centre are asymptotically Friedmann at $z = 0$.

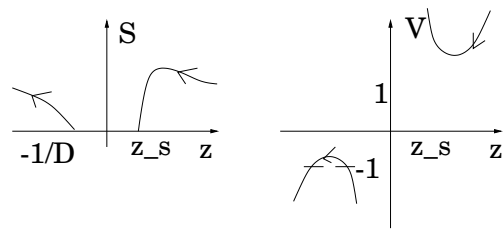


FIG. 9: The form of $S(z)$ and $V(z)$ for the recollapsing asymptotically quasi-static solutions which contain two singularities, one of which is naked. This shows the case $V_{\max} > -1$ and $V_{\min} > 1$. Both this case and the case with $V_{\max} < -1$ and $V_{\min} < 1$ have the conformal diagram of Fig. 5 except that the big bang singularity is at $z = -1/D$ instead of $z = \infty$.

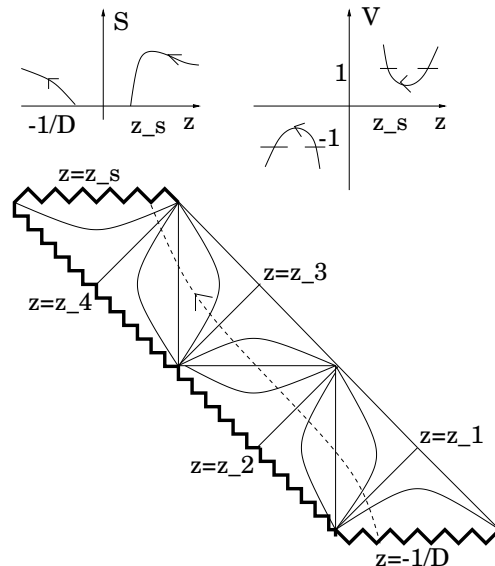


FIG. 10: The form of $S(z)$ and $V(z)$ for the recollapsing asymptotically quasi-static solutions which contain two naked singularities, together with the conformal diagram. The structure is sSfTpSfTpSs.

C. The asymptotically Minkowski solutions with $\alpha > \frac{1}{5}$

There are two families of asymptotically Minkowski solutions in the $z > 0$ regime and both are physical only for $\alpha > \frac{1}{5}$. Equivalent (time reversed) solutions exist in the $z < 0$ regime but we do not discuss these explicitly.

A) The first family is described by two parameters and has $V \rightarrow 1$, $S \rightarrow \infty$ and $\mu \rightarrow 0$ at some *finite* value $z = z_*$. In this limit,

$$\dot{V}/V = -(5\alpha - 1)/(1 - \alpha). \quad (13)$$

This family is illustrated in Fig. 13. Although the value of z is finite at z_* , the Schwarzschild radial distance ($R = rS$) is infinite, as is clearly seen in the $S(z)$ diagram. These are the “explosive solutions” of Ori and Piran [1], in which the fluid velocity approaches the speed of light,

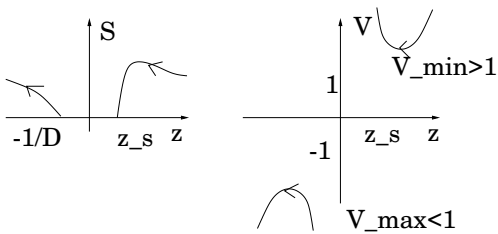


FIG. 11: The form of $S(z)$ and $V(z)$ for the recollapsing asymptotically quasi-static solutions which contain no naked singularities. The conformal diagram is the same as in Fig. 6, with structure sSs.

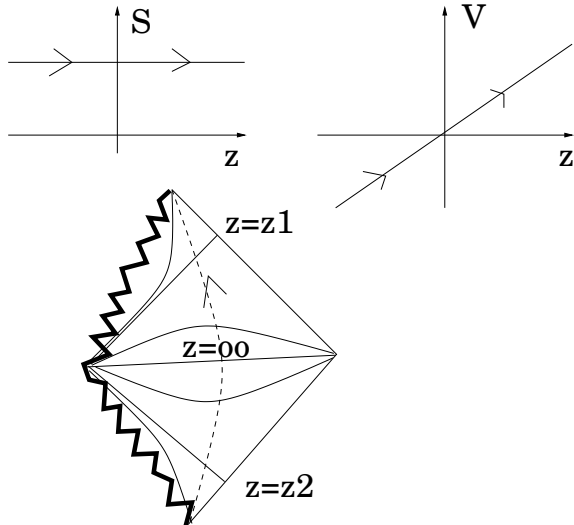


FIG. 12: The form of $S(z)$ and $V(z)$ for the exact static solution, together with the conformal diagram. The structure is sTfSfTs.

leaving null data for flat spacetime on an outgoing null cone.

B) The second family is described by one parameter and has $V \rightarrow V_* > 1$, $S \rightarrow \infty$ and $\mu \rightarrow 0$ as $z \rightarrow \infty$. The expression for V_* is

$$V_* = \frac{\alpha(\alpha + 1) + \sqrt{\alpha(\alpha^3 - \alpha^2 + 3\alpha + 1)}}{1 - \alpha}. \quad (14)$$

This family is illustrated in Fig. 14. Note that the V_* decreases as α decreases and reaches 1 when $\alpha = 1/5$.

In both cases, the limit $S \rightarrow \infty$ can be regarded as corresponding to an infinitely dispersed state, analogous to the late stage of an open Friedmann model. Also both families of solutions have $m/R \rightarrow 0$ in the asymptotic limit. The mass m itself tends to a finite value in case A but to zero in the case B. It is important to realize that these solutions are not asymptotically flat in the usual sense. Rather, they are perfect-fluid spacetimes for which the Minkowski geometry is obtained asymptotically along certain coordinate lines. This is reminiscent of the open Friedmann solution, which asymptotically

approaches the Milne model along certain time lines.

As can be seen in Figs. 13 and 14, both families contain solutions that can be connected either to the origin $z = 0$ (via a sonic point) or to a singularity (for which $S \rightarrow 0$ at some finite value z_s). The former are of type T or ST and correspond to singularity-free models which collapse and then bounce at some finite density into another expansion phase. The latter are of type S and collapse to a singularity without passing through a sonic point. We therefore have four situations. The bouncing 2-parameter case is illustrated in the left conformal diagram of Fig. 13. The conformal structure is very similar to the Minkowski case and can indeed be extended to a solution whose conformal structure is exactly like Minkowski if one adds another Minkowski patch to the top-left corner (shown dotted). There is a point singularity at $r = t = 0$. Since $\mu r^2 = 0$ at $z = z_*$, there is a singularity only where $r = 0$. The conformal diagram for the collapsing 2-parameter case is shown on the right of Fig. 13. This could also be attached to a Minkowski region (shown dotted), in which case it is similar to the conformal diagram in Fig. 7. It might also in principle be patched on to the top corner of the left conformal diagram. The 1-parameter case is illustrated in Fig. 14. Although $V = V_* > 1$ is finite as $z \rightarrow \infty$, the surface $z = \infty$ is not actually spacelike but consists of two null branches. As shown in appendix B, one of them is an outgoing null surface at finite distance – as in the type A solutions, it is possible to glue it onto Minkowski here – and the other branch is I_+ .

Note that there is a 1-parameter family of singular solutions for each value of z_s . Most of these will be asymptotic to either a type-A asymptotically Minkowski solution or a quasi-static solution. However, for sufficiently large values of z_s , there will also be one type-B asymptotically Minkowski solution and one asymptotically Friedmann solution. The limiting value of z_s is the same in each case, reflecting the fact that the conditions at large values of z have little influence on what happens near the singularity.

D. Asymptotic Kantowski-Sachs solutions

The final class of models is associated with the Kantowski-Sachs solution. For each α there is a unique self-similar Kantowski-Sachs solution and there also exists a 1-parameter family of solutions asymptotic to this at both large and small values of $|z|$. Solutions with $-1/3 < \alpha < 1$ are probably unphysical because the mass is negative and they are also tachyonic for $0 < \alpha < 1$. Solutions with $-1 < \alpha < -1/3$ avoid these unsatisfactory features. Although such equations of state violate the strong energy condition, they could well arise in the early Universe due to inflation or particle production effects.

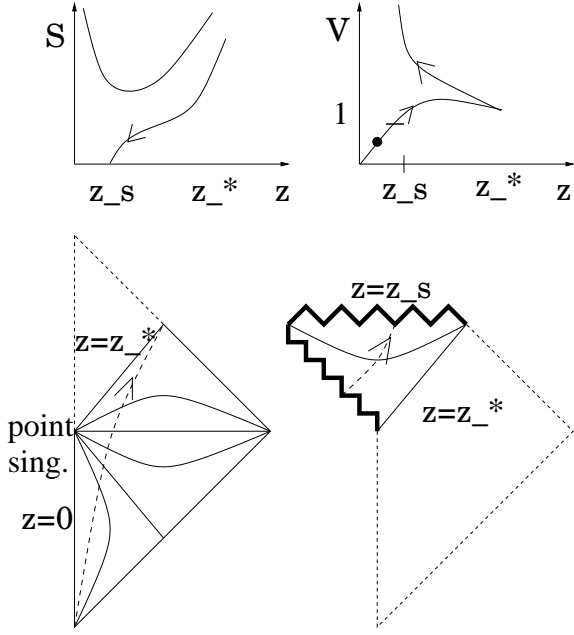


FIG. 13: The form of $S(z)$ and $V(z)$ for the 2-parameter bouncing and collapsing asymptotically Minkowski solutions, together with the conformal diagram. There are two solutions which are geodesically incomplete. Each of them can separately be continued as Minkowski, and this is shown by the thin dashed line. One fluid world line is shown as a thicker dashed line. The two solutions can also be glued together at $z = z_s$. Note that in this case $z = z_*$ is a fan on one side and a splash on the other, because $V(z)$ has a minimum at $V = 1$ there, rather than crossing $V = 1$. The causal structure of the incomplete spacetime on the left is rTfSfTf. The causal structure of the incomplete spacetime on the right is pSs.

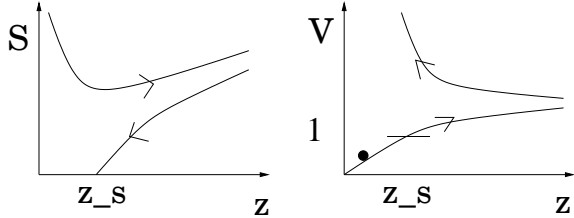


FIG. 14: The form of $S(z)$ and $V(z)$ for the 1-parameter bouncing and collapsing asymptotically Minkowski solutions. The conformal diagram and the causal structure are the same as in Fig. 13, with z_* replaced by $z = \infty$.

In the asymptotically KS solutions, $S \propto z^{-1}$ and V is also a decreasing power of z for $-1 < \alpha < -1/3$. Thus both S and V decrease to 0 as $z \rightarrow \infty$, as indicated in Fig. 15. This means that there is a timelike singularity at $t = 0$ and there is no spacelike infinity since R depends only on t . The conformal diagram is therefore as indicated in Fig. 15. The KS solution can be obtained from the static one by changing the value of α and interchanging r and t ; this explains why the conformal diagram of the KS solution resembles one half of that of the static solution [3].

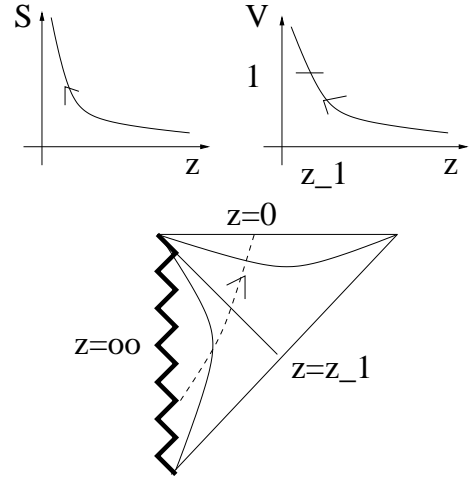


FIG. 15: The form of $S(z)$ and $V(z)$ for the asymptotically Kantowski-Sachs solutions with $-1 < \alpha < -1/3$, the only physical ones. The causal structure is sTfSr.

V. CRITICAL SOLUTIONS AND SHOCKS

Critical phenomena in gravitational collapse arise during the evolution of asymptotically flat regular initial data that are close to the threshold between black hole formation and dispersion. Such near-critical data approach a universal intermediate attractor before they either form a black hole or disperse. In dynamical systems terms, this “critical solution” is an attractor of codimension one, whose stable manifold separates the phase space into solutions that form a black hole and those that disperse. In terms of perturbation theory, it must have exactly one unstable linear perturbation mode, such that adding any amount of the unstable mode with one sign eventually drives the solution to collapse, and adding any amount with the opposite sign drives it to dispersion.

The property of being at the boundary of collapse can be realized in two ways: either the solution is static, corresponding to an unstable star, or it is self-similar, corresponding to scale-invariant collapse to a point. In “type II” critical phenomena the critical solution is self-similar (either CSS or DSS), and the black hole mass m_{bh} as a function of the initial data exhibits a power-law scaling of the form

$$m_{\text{bh}} \sim (p - p_*)^\gamma. \quad (15)$$

Here p is any one parameter of the initial data that is being varied while all other parameters remain fixed, and p_* is its critical value, such that data with $p > p_*$ form a black hole, while data with $p < p_*$ disperse. The critical exponent γ is independent of the initial data, and depends only on the symmetry of the system under consideration and type of matter. It can be related to the growth rate of the unstable mode of the critical solution [9, 10].

Type II critical phenomena were first described by Choptuik [11] for the spherically symmetric massless scalar field. Abrahams and Evans [12] described type II critical phenomena for axisymmetric vacuum gravity. In both cases the critical solution is DSS. The critical collapse of a spherically symmetric perfect fluid, the system which interests us here, was first investigated by Evans and Coleman [13] and is CSS. Many other systems were investigated subsequently and it seems that critical phenomena are generic. For a recent review, see [9].

Critical phenomena arise from any smooth initial data, in particular from analytic initial data. The time evolution of these data is analytic until the singularity occurs. (In fluids, it is possible that a shock could form first, but empirically this is not the case.) The critical solution, if it is to approximate such evolutions, must share this analyticity property. A spherically symmetric CSS fluid critical solution in particular must be analytic at the center to the past of the singularity and at the sonic point to the past of the singularity. These requirements define a boundary value problem between the regular center and the first sonic point. This problem admits a countable family of solutions which are parameterized by the number of zeros of the radial velocity V_R . The critical solution (with one unstable mode) turns out to be the one with a single zero [14], with the fluid ingoing in a central region and outgoing in the exterior. These solutions were first obtained numerically in [13] for $\alpha = 1/3$, in [10, 15] for $0 < \alpha < 0.89$, and in [16] for $0 < \alpha < 1$.

Type II critical solutions have renewed interest in the study of self-similar solutions in general relativity. We have seen that every self-similar spacetime has a strong curvature singularity $s = 0$ (unless it is flat). In critical solutions this singularity is naked, in the sense that light rays can escape from regions of arbitrarily high curvature with a finite redshift. In the collapse of near-critical initial data, the solution is well-approximated by the critical solution down to a lower cut-off scale of $s \sim |p - p_*|$. Consequently the maximal value of the Kretschmann scalar that can be seen is $|p - p_*|^{-4}$. In the limit in which the parameter p is tuned to its critical value p_* , the naked singularity of the critical solution is seen. Therefore the naked singularity of the critical solution is produced from a set of codimension one in the space of smooth and asymptotically flat data.

Because the critical solution is determined by analyticity at the center in the past of the singularity and the past sound cone of the singularity, its continuation from the past sound cone is unique up to the future light cone of the singularity, which acts as a Cauchy horizon. We shall briefly discuss possible continuations beyond the Cauchy horizon, but this is likely to be irrelevant to gravitational collapse because quantum gravity effects are expected to become important at very high curvature.

The nature of the critical solution in spherical perfect fluid collapse with the equation of state $p = \alpha\mu$ has been

discussed by CCGNU [8]: For $0.28 < \alpha < 1$ the critical solution is of the asymptotically Minkowski A type, and for the special value $\alpha \simeq 0.28$ it is asymptotically Minkowski type B. In both cases the spacetime structure is given by the left conformal diagram in Fig. 13.

The simplest continuation beyond the Cauchy horizon at $z = z_*$ would be a wedge of flat empty spacetime, as indicated by the thin dashed line in the left diagram in Fig. 13. In this case, the CSS singularity is a single point. The Ricci scalar at the center diverges as t^{-2} for $t < 0$, and vanishes for $t > 0$.

Another possible continuation would be the right conformal diagram in Fig. 13. From the general arguments in Section III we see that such continuations form a 2-parameter family. In this case the singularity has a null branch which is completely covered by a spacelike branch. Note that this continuation is filled by fluid particles that emerge from the null branch of the singularity and end at the spacelike branch. It could therefore be described as a black hole expanding at the speed of light or as a baby universe. A distant observer would see the t^{-2} divergence of the curvature at the center, but would be swallowed by the expanding black hole at $t = 0$.

For $0 < \alpha < 0.28$, the critical solution is asymptotically quasi-static, but its causal structure differs from the asymptotically quasi-static solutions that we have discussed already. The reason is that it crosses the sonic surface twice. The structure of the critical solutions with $0 < \alpha < 0.28$ up to the second sonic point is TST and shown in Fig. 16. We call the second sonic point the sonic horizon, in analogy to the Cauchy horizon of the singularity. CCGNU find that at the sonic horizon the critical solution reaches the sonic surface away from the sonic line. As discussed in Appendix A, this means that it cannot be continued as a C^0 solution, so the density gradient and velocity gradient become infinite at the sonic horizon.

This suggests that before the solution curve reaches the sonic surface a shock occurs. It must be to the future of the Cauchy horizon and to the past of the z -line where the CSS ansatz breaks down. Therefore its location curve $r = r_{\text{sh}}(t)$ is bounded by $z_{\text{ch}} < r_{\text{sh}}(t)/t < z_{\text{sp}}$. The most natural assumption compatible with this is that the shock location is also self-similar, or $r_{\text{sh}}(t)/t = z_{\text{sh}} = \text{const}$. Such solutions have been investigated by Cahill and Taub [17], and we need only summarize their results here with our notation.

Given a CSS solution with a shock at z_0 , the solution on one side uniquely determines the solution on the other side. The Israel matching conditions reduce in spherical symmetry to continuity of the Hawking mass m and the area radius R , so it follows that $M = m/R$ is continuous. We can also use the scale invariance of CSS solutions to impose the gauge condition that the coordinate r be continuous. Continuity of R is then equivalent to continuity of S . The Rankine-Hugoniot conditions for the fluid give

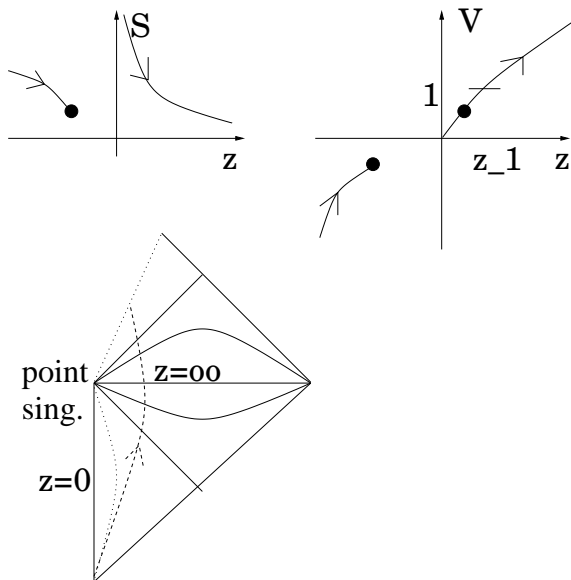


FIG. 16: The form of $S(z)$ and $V(z)$ and the conformal diagram for the critical solutions with $0 < \alpha < 0.28$. The spacetime cannot be continued through the second sonic point as a CSS and continuous solution, but it can be continued through a shock. The two dashed lines are the sonic points, marked with dots in the S and V plots.

V and

$$W \equiv \mu R^2 = \frac{\eta S^2}{8\pi G} \quad (16)$$

on one side in terms of their values on the other side (Eqs. (6.23-24) of [17]). The complete matching conditions are

$$S_+ = S_-, \quad (17)$$

$$M_+ = M_-, \quad (18)$$

$$V_+^2 = \frac{\alpha^2}{V_-^2}, \quad (19)$$

$$W_+ = \frac{(V_-^2 - \alpha^2)W_-}{\alpha(1 - V_-^2)}. \quad (20)$$

Note that $|V| < \sqrt{\alpha}$ on one side and $V > \sqrt{\alpha}$ on the other. One also requires $|V| > \alpha$ on both sides for W to be positive. Therefore V_- is restricted by the condition $\alpha < |V_-| < \sqrt{\alpha}$. We thus have a 1-parameter family of possible continuations parameterized by V_- in this range, so the existence of the shock adds one free parameter, namely z_0 , just like a nodal sonic point. In the strong shock limit $V_-^2 \rightarrow \alpha^2$ we obtain $W_+ \rightarrow 0$ and $V_+^2 \rightarrow 1$, but the energy density measured by a timelike observer, $\mu_+/(1 - V_+^2)$, remains finite in this limit. In the limit $V_-^2 = \alpha$ the shock disappears, with $W_+ = W_-$ and $V_+ = V_-$.

VI. CONCLUSIONS

In this paper we have established the conformal structure of all possible spherically symmetric CSS solutions, independently of the Einstein equations. We have then listed all possible conformal structures if the matter is a perfect fluid with equation of state $p = \alpha\mu$. This includes the solutions associated with critical phenomena in gravitational collapse.

Our kinematical discussion is based on the ideas of Nolan [2] and some of our diagrams were first drawn by Ori and Piran [1]. However, Nolan's kinematical discussion is restricted to spacetimes compatible with ingoing null dust matter, and his use of the Einstein equations is limited to imposing a positive energy condition. Ori and Piran only consider spacetimes with a regular center in the past.

The main limitation of our discussion is that we have excluded solutions with shocks. Such solutions may have more free parameters than differentiable ones and they may even admit additional conformal diagrams. Also we have only considered CSS continuations of the critical solutions beyond their Cauchy horizon but this is probably not a serious restriction because the continuation must be asymptotically CSS at small scales.

By drawing the conformal diagrams we have been able to elucidate the nature of some previously obscure CSS solutions. In particular, the conformal structure of the asymptotically Minkowski solutions of type A and type B are the same, and the CSS solutions that describe a black hole forming in an open universe have a null singularity, which can either be completely covered by the black hole singularity (see Fig. 13 on the right) or covered only partly.

An interesting result is that, while the singularity may have past branches from which fluid worldlines emerge and future branches where they end, these branches must be connected by a null branch. All parts of the singularity are therefore topologically connected. The recollapsing models, for example, do not have the conformal diagram of the closed Friedmann universe, with disjoint big bang and big crunch singularities, but one of the conformal diagrams indicated in Fig. 5, Fig. 6 and Fig. 10.

Reviewing earlier work [7], we have placed the critical solutions which arise in gravitational collapse within our general classification. These solutions are analytic and unique up to the Cauchy horizon of the CSS singularity. Intuitively one might expect the continuation of the critical solution to be non-unique because it depends on information coming out of the naked singularity. As information in spherically symmetric fluid solutions travels only at the speed of sound (because there are no gravitational waves), one would expect the spacetime to be non-unique beyond the sonic horizon of the singularity. However, contrary to this intuition, we have shown that the critical solution is non-unique even before the sonic

horizon, at the Cauchy horizon.

Acknowledgments

We would like to thank J. M. Martín-García for interesting discussions and for the use of his numerical code to compute the critical solutions.

APPENDIX A: THE SONIC SURFACE

Bicknell and Henriksen [6] have expanded a generic solution around a point in the sonic line in terms of a parameter u along the solution curve (M, S, z, η) . To linear order they find

$$(\delta M, \delta S, \delta z, \delta \eta)(u) = \alpha_1 e^{\lambda_1 u} \mathbf{V}_1 + \alpha_2 e^{\lambda_2 u} \mathbf{V}_2 \quad (\text{A1})$$

where the eigenvalues $\lambda_{1,2}$ and eigenvectors $\mathbf{V}_{1,2}$ are known, and $\alpha_{1,2}$ are free constants. By parameter counting, this linearized solution is generic. There are also two other eigenvectors with zero eigenvalues in the 4-dimensional (M, S, z, η) space. One takes the solution out of the constraint surface $c = 0$, and the other takes it along the sonic line. Their amplitudes can consistently be set to zero.

The nature of the solution depends crucially on $\lambda_{1,2}$, which are the solutions of a real quadratic equation. If they form a complex conjugate pair the point on the sonic line is called a focus. The formal solution (A1) is then complex and spirals around the sonic point in phase space. No solution crosses the sonic surface at this point.

If $\lambda_{1,2}$ are real with the same sign, the point on the sonic line is called a node. We may assume without loss of generality that $\lambda_1 < \lambda_2 < 0$. Then the sonic line is crossed as $u \rightarrow \infty$. Furthermore, as $u \rightarrow \infty$, $e^{\lambda_1 u}$ can be neglected compared to $e^{\lambda_2 u}$, and the implicit functions $M(z)$, $S(z)$, $\eta(z)$ are C^1 . Therefore a 1-parameter family of C^1 solutions crosses each point of the sonic line. All these solutions have the same tangent at the sonic point. The solution with $\alpha_1 = 0$ from this family is analytic. There is also an isolated analytic solution with $\alpha_2 = 0$.

If $\lambda_{1,2}$ have opposite signs, the point on the sonic line is called a saddle. Without loss of generality, we assume $\lambda_1 < 0 < \lambda_2$. Then there are only two isolated solutions that cross the sonic surface: the solution with $\alpha_1 = 0$ as $u \rightarrow -\infty$ and the solution with $\alpha_2 = 0$ as $u \rightarrow \infty$. Both solutions are analytic.

The sonic line can be parameterized by z . It then turns out that the points $0 < z < z_1$ are saddles, $z_1 < z < z_2$ are nodes, $z_2 < z < z_3$ are focal points, and $z_3 < z < \infty$ are nodes again, where $z_{1,2,3}$ are known functions of α [3]. The static solution has a sonic point between z_1 and

z_2 , while the flat Friedmann solution has a sonic point above z_3 .

The two nodal segments of the sonic line are attractors, and are crossed by generic 2-parameter families of solutions. The saddle segment of the line is crossed only by a 1-parameter family of solutions. Generic solutions therefore miss the saddle segment of the sonic line and reach the sonic surface away from the sonic line. Expanding around a point in the sonic surface but off the sonic line, where $V^2 = \alpha$ but $g \neq 0$, we find to leading order that

$$\delta M \simeq a \delta z, \quad (\text{A2})$$

$$\delta S \simeq b \delta z, \quad (\text{A3})$$

$$\delta \eta \simeq \pm \sqrt{2g \left(\frac{\partial V^2}{\partial \eta} \right)^{-1}} \delta z, \quad (\text{A4})$$

$$\delta V \simeq \pm \sqrt{2g \frac{\partial V^2}{\partial \eta}} \delta z \quad (\text{A5})$$

This point on the sonic surface is reached by two solution curves from one side, but there is no solution curve that reaches it from the other side. Note also that, because $R = rS$ and $8\pi G\mu = r^{-2}\eta$, the comoving physical density gradient $d\mu/dR$ and velocity gradient dV/dR diverge.

APPENDIX B: ASYMPTOTICALLY MINKOWSKI TYPE B

From Eq. (3.43) of [3] we see that as $z \rightarrow \infty$, the space-time metric is approximately of the form

$$ds^2 = -A^2 z^{2a} dt^2 + B^2 z^{2b} dr^2 + S_0^2 r^2 z^{2c} d\Omega^2 \quad (\text{B1})$$

where

$$B/A = V_*, \quad a - 1 = b = 1/(V_*^2 - 1), \quad c = 1/(V_* - 1). \quad (\text{B2})$$

where V_* is given by Eq. (14). This (approximate) metric can be written as

$$ds^2 = -C du dv + S_0^2 v^2 d\Omega^2 \quad (\text{B3})$$

where $C > 0$ is a known constant, and

$$u = -rz^{-1/(1+V_*)}, \quad v = rz^{1/(V_*-1)}, \quad (\text{B4})$$

are negative and positive, respectively. Contrary to the claim in [3], this metric is not Minkowski. From the form of the metric, it is clear that u and v are affine parameters of null geodesics. $z = \infty$ has two branches: $u = 0$, which is therefore at finite affine parameter distance, and $v = \infty$, which is at infinite affine parameter distance. The former is a regular surface and the spacetime can be continued there. The latter is I^+ . Fluid worldlines $r = \text{const}$ end up at $(u = 0, v = \infty)$. Note that this point is not i_0 : observers that resist the outward fluid pressure

can cross the surface $u = 0$. It should be stressed that metrics (B1) and (B3) are only approximate. Were they exact, the mass function would be $m/R = 1/2$ because

$R = S_0 v$. However, non-leading terms actually show that $m/R \rightarrow 0$ in the limit $z \rightarrow \infty$.

-
- [1] A. Ori and T. Piran, Phys. Rev. Lett. **59**, 2137 (1987).
 [2] B. C. Nolan, Class. Quant. Grav. **18**, 1651 (2001).
 [3] B. J. Carr and A. A. Coley, Phys. Rev. D **62**, 044023 (2000).
 [4] K. Lake and T. Zannias, Phys. Rev. D **41**, 3866 (1990).
 [5] C. Gundlach and J. M. Martín-García, Global structure of Choptuik's critical solution in scalar field collapse, in preparation.
 [6] G. V. Bicknell and R. N. Henriksen, Astrophys. J. **225**, 237 (1978).
 [7] B. J. Carr, A. A. Coley, M. Goliath, U. S. Nilsson, and C. Uggla, Class. Quant. Grav. **18**, 303 (2001).
 [8] B. J. Carr, A. A. Coley, M. Goliath, U. S. Nilsson, and C. Uggla, Phys. Rev. D **61**, 081502 (2000).
 [9] C. Gundlach, Living Reviews in Relativity **2**, 4 (1999), published electronically at <http://www.livingreviews.org>.
 [10] T. Koike, T. Hara, and S. Adachi, Phys. Rev. Lett. **74**, 5170 (1995).
 [11] M. W. Choptuik, Phys. Rev. Lett. **70**, 9 (1993).
 [12] A. M. Abrahams and C. R. Evans, Phys. Rev. Lett. **70**, 2980 (1993).
 [13] C. R. Evans and J. S. Coleman, Phys. Rev. Lett. **72**, 1782 (1994).
 [14] T. Harada, Class. Quant. Grav. **18**, 4549 (2001).
 [15] D. Maison, Phys. Lett. B **366**, 82 (1996).
 [16] D. W. Neilsen, Class. Quant. Grav. **17**, 733 (2000).
 [17] M. E. Cahill and A. H. Taub, Comm. Math. Phys. **21**, 1 (1971).